EAGE

ECMOR XV

Mo Gra 12

Micro-continuum Formulation for Modelling Dissolution in Natural Porous Media

CS Soulaine* (Stanford University) & H.A. Tchelepi (Stanford University)

SUMMARY

Advances in imaging technologies and high-performance computing are making it possible to perform Direct Numerical Simulation (DNS) of flow processes at the pore scale; nevertheless, the restrictions on the physical size of the sample (porous rock) that can be fully resolved using Navier-Stokes-based DNS are quite severe. Even for samples on the order of a cm3, the complexity of the spatial heterogeneity of the pore space precludes Navier-Stokes-based DNS. To deal with this challenge of having a wide range of length scales – even for `small' systems, we describe a micro-continuum formalism, whereby locally averaged equations and associated coefficients can be used to model the effects of scales that are below instrument resolution and/or DNS capability. A hybrid modeling framework based on the Darcy-Brinkman-Stokes (DBS) equation is employed. In this approach, a single equation is applicable for flow in `channels' (so-called `free flow') and in porous media (solid-fluid aggregates). A unified simulation framework for multi-physics problems of mass and heat transport in natural porous media based on a hybrid Darcy-Brinkman-Stokes approach is described. We discuss two specific applications: minerals dissolution in CO2-brine systems, and dissolution instabilities (worm-holing phenomena) associated with the acidizing treatment of carbonate formations.

Introduction

Dissolution of solid minerals appears in many subsurface transport processes. Application areas relate to subsurface hydrology, reservoir engineering, and CO_2 sequestration. In the acidizing process, acid is injected to enhance the conductivity around the wellbore by dissolution and creation of wormholes. Another example concerns the sequestration of CO_2 in deep saline aquifers. The injected supercritical CO_2 flows as a separate fluid phase that is immiscible with the resident brine. Complex interfacial (fluid-fluid and fluid-solid) dynamics that depend strongly on the wettability of the mineral surface can lead to the trapping of CO_2 ganglia in the pore space. CO_2 from the supercritical phase dissolves in the aqueous (brine) phase to form carbonic acid, which lowers the pH of the brine as the carbonic acid dissociates into bicarbonate ions [Steefel et al. (2013); Cohen and Rothman (2015)]. The acid ions are then transported by advection and diffusion to the mineral surface where the dissolution and precipitation of the minerals can occurs [Molins et al. (2014)]. Calcite dissolution is one of the important dissolution reactions that occurs during sequestration. These dynamic processes associated with the injection and sequestration of CO_2 into deep saline aquifers can produce significant changes in the pore space, and this can lead to significant changes in macroscopic properties such as permeability and porosity [Rathnaweera et al. (2016)]. Dissolution effects must also be accounted for in order to properly assess the long-term integrity of the caprock in many settings.

Dissolution patterns take different forms according to the flow conditions and the mineral properties. For example, at low enough injection rates, the characteristic time scale for reaction can be quite small compared with that for acid transport; in this case, the acid gets consumed as it invades the porous formation around the wellbore, which leads to limited propagation of the acid. At higher flow rates, however, instabilities begin to develop, which can evolve into ramified wormholes [Daccord and Lenormand (1987); Fredd and Fogler (1998); Golfier et al. (2002)]. Classical models use Representative Elementary Volume (REV)-based equations to describe such a system. Important challenges associated with such approaches relate to the relationship between porosity and permeability and the representation of the dissolution rate. Changes in the pore space depend on the details of the competition between the transport and the reactions, which ultimately determine the evolution of permeability and porosity. As a result, it is difficult to come up with a universal formulation of the dissolution rate at the scale of the REV (i.e., aggregate of solid and fluids). The reactive surface available to the acid species is a critical parameter for macroscopic (REV) dissolution models. This is a very difficult quantity to obtain a-priori, since it is a complex function of the local flow conditions. Indeed, as illustrated in Figure 1, the flow distribution in the pore space of a sandstone replica (see Roman et al. (2015) for the details) reflects the presence of preferential-flow regions and some effectively dead-end zones. In such configurations, the species transport may be dominated by convection in the fast regions and by diffusion in the slow zones. Hence, for high Péclet numbers, the acid ions cannot reach the surface mineral in the dead-end zones. Moreover, natural rocks usually consist of multiple minerals, such as calcite, clay, quartz, dolomite, and pyrite. The different minerals have very different reaction rates, and that adds to the challenge of REV-scale dissolution models. In this paper, we study dissolution of minerals at the pore-scale where the solid skeleton is fully described. This serves as a basis for assessing the impact on the evolution of the porosity and permeability.

Several techniques have been proposed since the pioneering work of Békri et al. (1995), which entailed solving the Stokes equations combined with a 'pixel-based' dissolution rate. Techniques using the Arbitrary-Lagrangian-Eularian (ALE) framework solve the full physics at the pore scale on an Eularian grid, *i.e.* Navier-Stokes equations, transport equation and chemical reaction at the solid boundaries, and then move the grid in time [Luo et al. (2012); Oltéan et al. (2013)]. ALE techniques are very accurate, but they are limited to a few grains only and cannot be used to simulate the evolution of the pore space for large-scale systems. These methods can serve, however, as a reference for validating other numerical approaches. Alternative methods use the level-set function to transport the fluid-solid interface with immersed reactive boundaries on an Eularian grid during the dissolution processes [Li et al. (2010); Huang and Li (2011); Xu et al. (2012); Trebotich and Graves (2015)]. Other works rely on Lattice Boltzmann methods for reactive mass transfer in porous media [Kang et al. (2003); Szymczak and Ladd (2004, 2009); Huber et al. (2014); Chen et al. (2014); Kang et al. (2014)]. Methods based

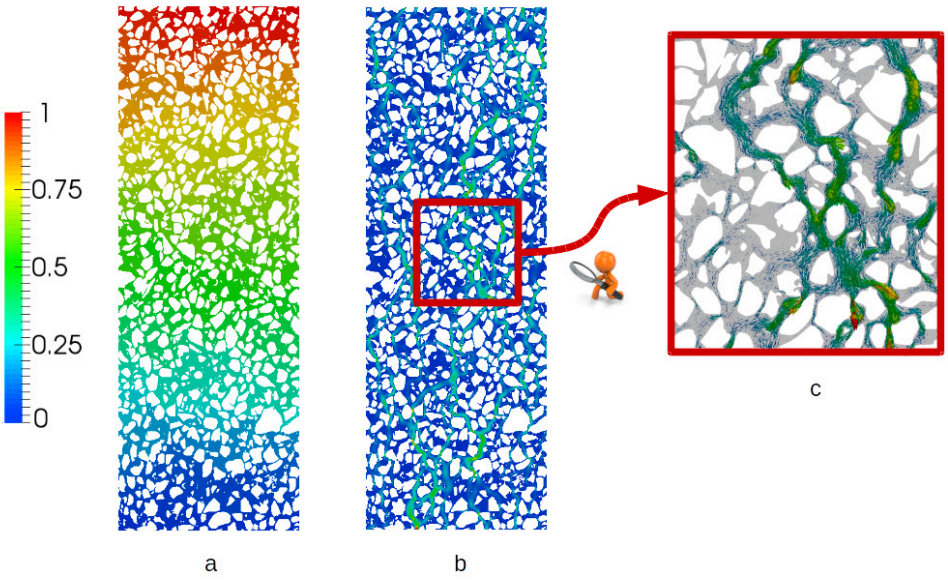

Figure 1 *Plot of a Stokes simulation results in a sandstone replica. The resulting fields are normalized by the highest value.* (a) *Pressure field,* (b) *Magnitude of the velocity field,* (c) *Velocity vectors in a zoom in.*

on the Darcy-Brinkman-Stokes (DBS) equation [Brinkman (1947)] for numerical modeling of dissolution processes in porous media have been proposed [Golfier et al. (2002); Luo et al. (2012, 2014); Guo et al. (2014); Luo et al. (2015); Soulaine and Tchelepi (2016)]. In the micro-continuum DBS approach [Soulaine and Tchelepi (2016); Soulaine et al. (2016)], the solid grains (matrix) are treated as porous media and differentiated from the void (fluid filled) region based on the volume-fraction of solid per cell, or control-volume. This Eulerian method employs a single equation to simulate Stokes flow in the void regions and Darcy's law for transport through the grains. In the classic micro-continuum models proposed by Golfier et al. (2002), a porous-media formulation with a non-equilibrium model is used for transport of the acid species in addition to chemical reactions with the solid minerals. The challenges to model the dissolution rate in the matrix are those associated with the porous media formalism: how to estimate the effective surface area; how does the dissolution rate depend on the flow conditions; how the mass-transfer coefficient(s) depend on on the Péclet (*Pe*) and Damköhler (*Da*) numbers. Here, we extend the micro-continuum (DBS) approach to simulate pore-scale dissolution phenomena. For numerical validation, we compare the micro-continuum approach with reference ALE-based solutions.

This paper is organized as follow. Next we introduce the mathematical and numerical models of the micro-continuum approach for dissolution at the pore scale. Then, we show how the model compares with ALE for single-grain dissolution. Following that, we use the DBS formalism to simulate dissolution in more complex pore structures, and we discuss the emergence of wormholes. We close with summary and conclusions.

Mathematical model

We introduce the mathematical model used to simulate dissolution processes in porous media at the pore scale. The approach is based on the model proposed by Golfier et al. (2002) to simulate the evolution of wormholes at the core scale. Instead of a full Navier-Stokes approach, the model adopts a micro-continuum formulation, whereby an arbitrary cut-off length is imposed; all the information regarding the

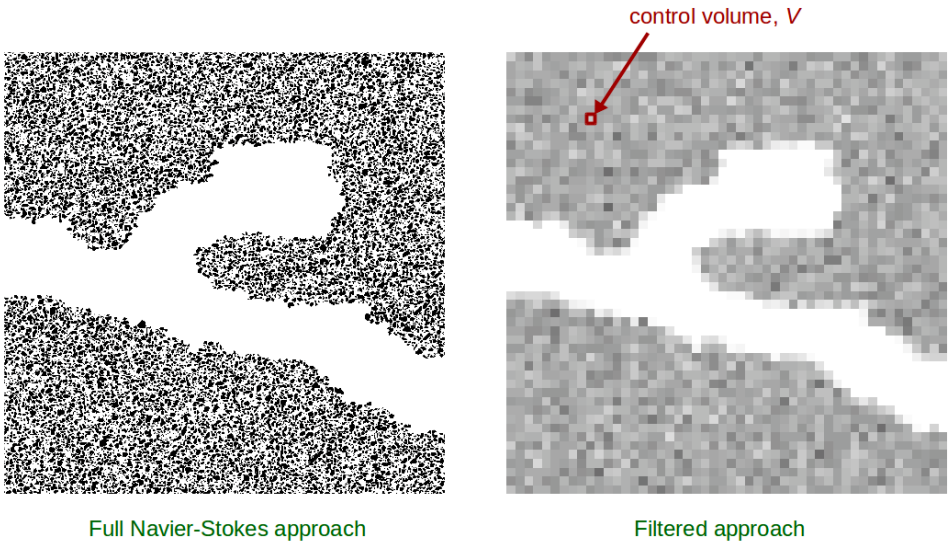

Figure 2 *Representation of the void using the full Navier-Stokes approach versus the filtering approach. In the full Navier-Stokes approach, all the solid grain are described explicitly. The flow is governed by the Navier-Stokes equations everywhere in the void, and a no-slip boundary is specified at the grain boundaries. In the filtering (micro-continuum) approach, a cut-off length is introduced by means of a control volume, V, and the void is represented by the volume fraction, ε_f. If $\varepsilon_f = 1$ (inside the large channel), the flow is governed by the Navier-Stokes equations; for intermediate values, $0 < \varepsilon_f < 1$, there are solid obstacles in the control-volume, and the flow is governed by Darcy's law. (Image from Soulaine and Tchelepi (2016))*

solid-fluid structure below this length-scale is filtered and modeled as a porous medium. Mathematically, this cut-off length is associated with a control volume, V, and all the quantities in the system are averaged over V. The control volumes (computational cells) that contain void only, also called clear-fluid, or free, zones, and those that contain (some) solid are differentiated by ε_f, which is the volume fraction of void space within control volumes. ε_f is a field with different values in the domain that range from 0 to 1. This filtering approach is illustrated in Figure 2. The free zone is denoted by $\varepsilon_f = 1$ where the flow is governed by the Navier-Stokes equations. For intermediate values, $0 < \varepsilon_f < 1$, we have an aggregate of solid and fluids in the control volume, and the flow is governed by Darcy's law. When $\varepsilon_f = 0$, the control-volume contains solid only, and there is no flow. Different from other micro-continuum models, the filtering formulation is used to simulate pore-scale physics; thus, only the bounding values $\varepsilon_f = 1$ and $\varepsilon_f = 0$ are used to differentiate the solid from the clear regions. In fact, to make the governing equations introduced below valid all over the computational domain, *i.e.* in the free and the solid regions, we assume that the cells describing solid regions always contain a tiny porosity, $\varepsilon_f = 0.001$.

Likewise, the other variables of the system are defined as averaged quantities over the control volume. The pressure and acid mass-fraction are intrinsic phase averages, $\bar{p}_f = \frac{1}{V_f}\int_{V_f} p_f dV$ and $\bar{\omega}_{f,A} = \frac{1}{V_f}\int_{V_f} \omega_{f,A} dV$, respectively, where V_f is the volume occupied by fluid in the control volume, and the velocity is defined as a superficial average, $\bar{\mathbf{v}}_f = \frac{1}{V}\int_{V_f} \mathbf{v}_f dV$, in agreement with Darcy's law.

The model is obtained from the integration of the Navier-Stokes momentum equation over a control volume in the presence of solid material [Vafai and Tien (1981, 1982); Hsu and Cheng (1990); Bousquet-Melou et al. (2002)]; the result is a single equation that is valid for both the free (fluid-filled) and the porous-medium physical domains. We have,

$$\frac{1}{\varepsilon_f}\left(\frac{\partial \rho_f \bar{\mathbf{v}}_f}{\partial t} + \nabla.\left(\frac{\rho_f}{\varepsilon_f}\bar{\mathbf{v}}_f\bar{\mathbf{v}}_f\right)\right) = -\nabla\bar{p}_f + \frac{\mu_f}{\varepsilon_f}\nabla^2\bar{\mathbf{v}}_f - \mu_f k^{-1}\bar{\mathbf{v}}_f, \tag{1}$$

where the locally averaged pressure $\bar{p}_f$ and velocity $\bar{\mathbf{v}}_f$ are the unknowns of the system. This equation

can be considered as an extension of the original Darcy-Brinkman-Stokes equation [Brinkman (1947)] with inertia in the free-zone and mass transfer between the two regions. Terms in the left-hand side denote the inertia. The first two terms in the right-hand side are the pressure gradient and the dissipative viscous force. The last term of the right-hand side of Eq. (1) represents momentum exchange between the fluid and solid phases, *i.e.* the Darcy resistance term, which vanishes in the free zone. In that case, Eq. (1) goes back to the Navier-Stokes form. The Darcy term is dominant in the solid (porous medium) region, so that the velocity is reduced to almost zero in this region. For low values of k, *e.g.*, around four orders of magnitude below the permeability of the porous structure - denoted by ε_f - the formulation essentially imposes a no-slip boundary condition at the fluid/solid interface [Angot et al. (1999); Khadra et al. (2000); Soulaine and Tchelepi (2016)].

During the dissolution process, the solid morphology evolves with chemical reactions at the minerals surface. Here, we consider only one mineral. Hence, the solid volume fraction in a control volume, ε_s, is an unknown of the system, and its evolution is governed by the mass-balance equation:

$$\frac{\partial \varepsilon_s \rho_s}{\partial t} = -\dot{m}, \tag{2}$$

where ρ_s is the solid density, and $\dot{m}$ is the rate of fluid/solid mass transfer. The latter has a non-zero value only at the fluid/solid interface. All the dissolved mass goes into the fluid phase, and the continuity equation for the fluid phase can be expressed as:

$$\frac{\partial \varepsilon_f \rho_f}{\partial t} + \nabla.(\rho_f \bar{\mathbf{v}}_f) = \dot{m}, \tag{3}$$

where ρ_f is the fluid density.

The solid (mineral) is dissolved by an acid denoted A. Since A is the only species in the fluid phase that reacts with the solid phase, we need to only solve for the concentration of A in the fluid mixture. The mass-balance equation averaged over the control volume is

$$\frac{\partial \varepsilon_f \rho_f \bar{\omega}_{f,A}}{\partial t} + \nabla.(\rho_f \bar{\mathbf{v}}_f \bar{\omega}_{f,A}) = \nabla.(\varepsilon_f \rho_f D_A^* \nabla \bar{\omega}_{f,A}) - \dot{m}_A, \tag{4}$$

where D_A^* denotes the effective diffusivity of species A into the fluid mixture, and $\dot{m}_A$ is the mass-exchange term with the solid minerals. As for $\dot{m}$, this mass transfer rate is non-zero only in presence of solid minerals. To account for tortuosity effects in the matrix, the effective diffusivity $\varepsilon_f D_A^* = \varepsilon_f^2 D_A$ is used, where D_A is the molecular diffusivity of acid into the fluid mixture [Wakao and Smith (1962)]. Note that in the free zone, $\varepsilon_f = 1$, and Eq. (4) takes the form of a classical advection-diffusion equation.

The mathematical statement formed by Eqs. (1)-(4) is valid over the entire Eularian computational grid whether the cell (control-volume) contains solids or not. In the solid regions, the drag force term leads to a near-zero velocity, which amounts to a no-slip boundary condition at the fluid/solid interface. During the dissolution process, the solid-fluid interface evolves, and the local permeability, k, has to be updated according to the solid distribution in the computational grid. Here, a Kozeny-Carman relation,

$$k^{-1} = k_0^{-1} \frac{(1-\varepsilon_f)^2}{\varepsilon_f^3}, \tag{5}$$

is used to estimate the local permeability as a function of the porosity. This allows the solver to switch automatically from Darcy to Navier-Stokes according to the cell porosity values: in the free zones, $\varepsilon_f = 1$ and then $k^{-1} = 0$. In this equation, k_0^{-1} is an input parameter that has to be small enough. In our experience, the value must be at least four orders of magnitude below the nominal permeability of the porous medium in order to simulate a no-slip boundary condition [Soulaine and Tchelepi (2016)].

The last ingredient in the model relates to the formulation of the mass exchange terms, $\dot{m}$ and $\dot{m}_A$. First, the rate of dissolved mass is obtained from a simple mass balance, $\dot{m} = \beta \dot{m}_A$ where β is a stoichiometric

coefficient. To calculate, $\dot{m}_A$, we assume a first-order reaction rate, so that the acid boundary condition at the solid surface is formulated as:

$$\mathbf{n}_{fs}.\left(\rho_f\left(\mathbf{v}_f-\mathbf{w}\right)\omega_{f,A}-\rho_f D_A\nabla\omega_{f,A}\right)=r\rho_f\omega_{f,A}, \tag{6}$$

where $\mathbf{n}_{fs}$ is the normal at the fluid/solid interface, $\mathbf{w}$ is the receding velocity of this interface due to the surface chemical reaction, and r is the reaction-rate constant. In our micro-continuum formulation, the flux boundary condition, Eq. (6) is not imposed directly along the edges of the computational grid, but instead, it is imposed as an immersed boundary condition. This is achieved by integrating Eq. (6) over a control volume. Hence, the flux can be expressed as:

$$\begin{aligned}\dot{m}_A &= \frac{1}{V}\int_{A_{fs}}\mathbf{n}_{fs}.\left(\rho_f\left(\mathbf{v}_f-\mathbf{w}\right)\omega_{f,A}-\rho_f D_A\nabla\omega_{f,A}\right)dA,\\ &= \frac{1}{V}\int_{A_{fs}} r\rho_f\omega_{f,A}dA,\\ &\approx a_v r\rho_f\bar{\omega}_{f,A},\end{aligned}$$

where a_v is the effective surface area in one cell of the Eularian grid. Since we use a micro-continuum formulation for pore-scale simulation, there is a sharp transition between the clear-fluid region and the solid region. Hence, we have $a_v=\left\|\nabla\varepsilon_f\right\|$. This relation is non-zero only at the immersed fluid/solid interface.

The mathematical problem introduced in this section was implemented in the open-source simulation platform OpenFOAM (http://www.openfoam.org). Equations (1) to (4) are first discretized using a finite-volume method and solved sequentially. The pressure-velocity coupling is handled by a predictor-corrector strategy based on the Pressure-Implicit with Splitting of Operators (PISO) algorithm [Issa (1985)]. The details of the numerical treatment are given by Soulaine and Tchelepi (2016).

Simulation results

We present several examples to illustrate the potential of a DBS based approach for modeling dissolution of solid minerals at the pore scale. First, we focus on the dissolution of a single grain and compare the results with simulations based on the Arbitrary-Lagrangian-Eularian framework. Then, we investigate the dissolution pattern in a more complex pore space.

Comparison with ALE simulations

Here, we compare the DBS model with ALE simulations, which we consider as reference solutions for pore-scale dissolution. The geometry is a $20\,\mu$m $\times$ 20mm two-dimensional box that contains a cylindrical pillar in the middle. We consider two grids for the DBS simulations, a 50×50 and a 100×100 Cartesian grids. The porosity is set to $\varepsilon_f=0.001$ for cells that lie in a cylinder of $7.6\,\mu$m in diameter centered in the middle of the domain. Hence, the edge of the pillar is approximated as a stair-wise surface. The top and bottom boundaries are set as impermeable fixed walls with no reaction. An acid solution with one-percent concentration is injected from the left side at a constant velocity $v_0=10^{-3}$ m/s for 30s. The right side is an outflow condition. The remaining input parameters are: $\mu_f=10^{-3}$ Pa.s, $\rho_f=1000\,\mathrm{kg/m^3}$, $\rho_s=2165\,\mathrm{kg/m^3}$, $D_A=10^{-9}\,\mathrm{m^2/s}$, $r=10^{-2}$ m/s and $k_0=10^{-15}\,\mathrm{m^2}$.

With the ALE formulation, only the void (fluid-filled) space is gridded. Hence, the cells that make up the solid pillar are removed, and tetrahedral cells are introduced to perfectly match the cylindrical geometry. Incompressible Navier-Stokes equations and a standard advection-diffusion equation are solved with OpenFOAM to transport the acid concentration in the computational domain. Different from the DBS approach, the ALE methodology requires the specification of boundary conditions at the solid surface, namely a no-slip boundary condition together with Eq. (6). Moreover, the surface reaction leads to dissolution of the solid phase, which means that the solid geometry evolves during the process. A mass balance yields the receding velocity, $\mathbf{w}$, at every point on the solid surface, $\mathbf{n}_{fs}.\mathbf{w}=-r\frac{\rho_f}{\rho_s}\omega_{f,A}$. The

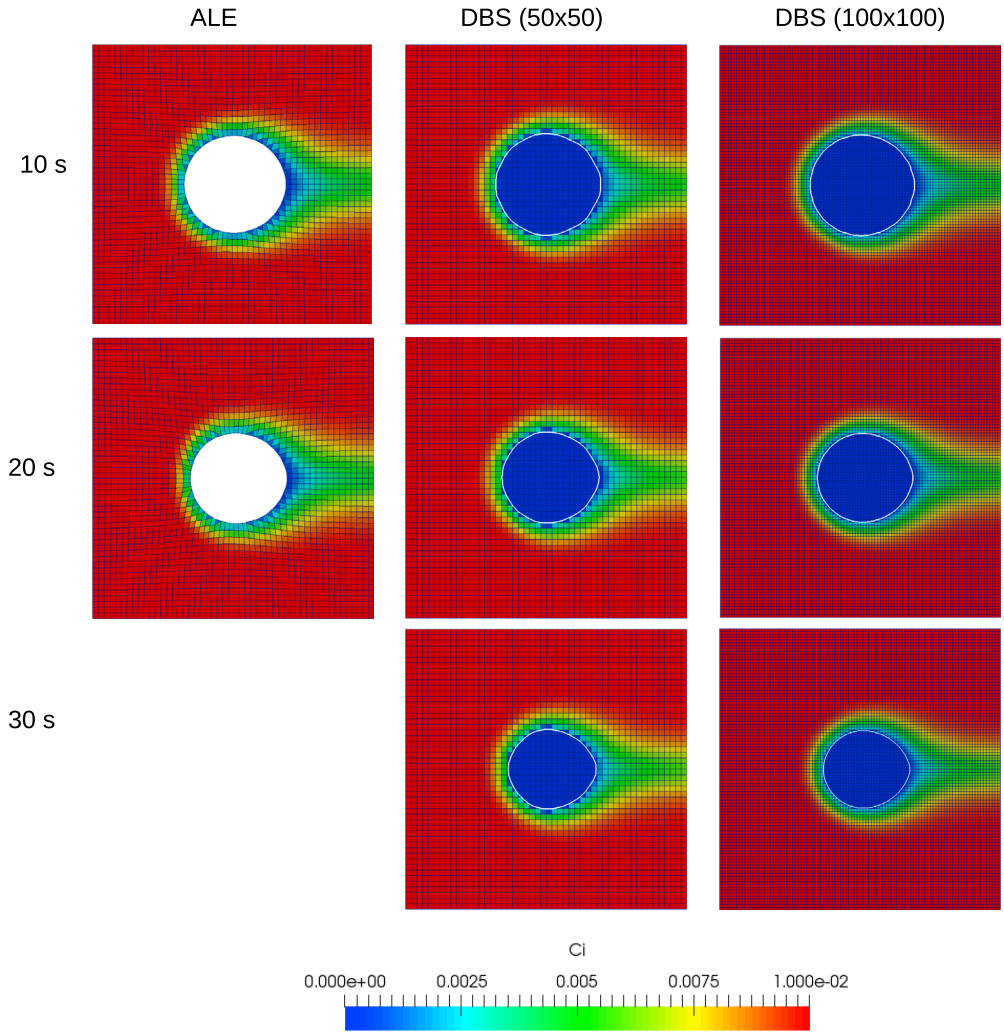

Figure 3 *Simulation results for the dissolution of a single pillar with ALE and DBS approaches. Both methods are in very good agreement and the DBS formulation reaches grid convergence.*

points of the grid at the reactive surface are moved accordingly, and a Laplacian equation is solved for the motion of all the points of the grid in order to have homogeneous deformations. After 20 s of simulated time, the mesh deformation reaches a point where cells with extreme aspect ratios are produced and the numerical simulation is halted.

Simulation results for the ALE and DBS approaches are plotted in Figure 3. We observe good agreement between the two methods. For both cases, the pillar deviates from its cylindrical shape during the dissolution process. This is the result of the complex interplay between transport and surface reaction. Indeed, the right side of the pillar acts as a dead-end zone for the flow where the acid concentration is quite low. Hence, the local dissolution rate in this area is less important than on the surface that faces the domain inlet, which explains the asymmetry. We note that the DBS results are converged solutions with respect to mesh refinement.

Pore-scale dissolution in a carbonate micromodel

We consider the dissolution in a complex pore space. The set-up details are described in Song et al. (2014) who conducted dissolution experiments in a real-rock micromodel directly etched in a carbonate. The model consists of multiple solid pillars that are roughly $500\,\mu\text{m} \times 500\,\mu\text{m}$, distributed homogeneously in a $24\,\text{mm} \times 7.2\,\text{mm}$ two-dimensional domain. The pillars are aligned and separated from each

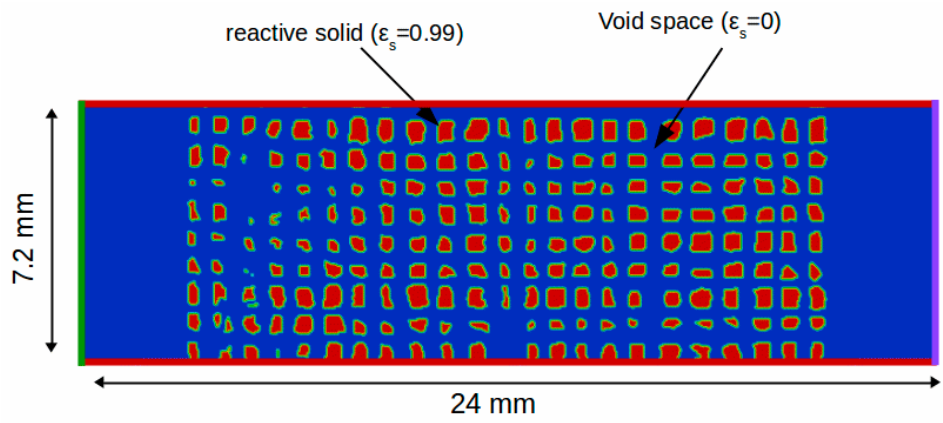

Figure 4 *Schematic of the real-rock micromodel. Blue corresponds to the void space ($\varepsilon_f = 1$) and red to the solid ($\varepsilon_f = 0.01$)*

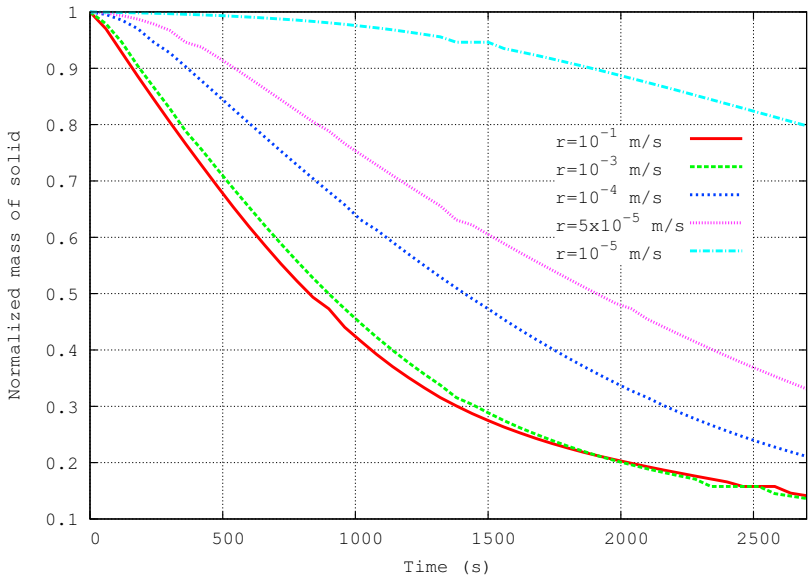

Figure 5 *Plot of the evolution of the total mass of solid in the domain for different reaction rates at the solid surface ranging from $r = 10^{-5}$ m/s to $r = 10^{-1}$ m/s.*

other by 300 μm wide vertical and horizontal channels as illustrated in Figure 4. The computational domain is gridded uisng 500×150 Cartesian grid. The top and bottom boundaries are impermeable, *i.e.* no-slip boundary conditions. One-percent acid solution is injected from the left of the domain at a constant velocity $v_0 = 10^{-3}$ m/s. The right side is an outflow condition. Additional properties include: $\mu_f = 10^{-3}$ Pa.s, $\rho_f = 1000\,\text{kg/m}^3$, $\rho_s = 2165\,\text{kg/m}^3$,$D_A = 10^{-9}\,\text{m}^2/\text{s}$ and $k_0 = 10^{-11}\,\text{m}^2$. These parameters correspond approximately to a Péclet number, $Pe \approx 300$.

We performed multiple simulations with reaction rates at the solid surface ranging from $r = 10^{-5}$ m/s to $r = 10^{-1}$ m/s. Similar to Song et al. (2014) experiments, we inject acid for 45 min. The time step was set to $\Delta t = 10^{-3}$ s. The simulations were performed using eight cores at the Stanford Center for Computational Earth & Environmental Sciences. The evolution of the total-mass of solid in the domain is plotted in Figure 5 for different reaction rates. We observe a nonlinear behavior when varying the value of r: for low Damköhler number, the total rate of dissolution starts slow, and then accelerates. On the other hand, for higher Da, the dissolution rate slows down during the entire simulation period. Figure 6 illustrates the evolution of the pore space for two different reaction rates, namely $r = 5 \times 10^{-5}$ m/s and $r = 10^{-3}$ m/s, after 10, 20, 30 and 40 min of the 1% of acid injection in the domain. The color

corresponds to acid concentration, and the white lines represent the boundaries of the pillars. We observe that the evolution of the pore space follows different patterns depending on the reaction rate at the solid surface. For the lower value of r, i.e., for a low Damköhler number, the characteristic time-scale for the chemical reaction is longer than the transport timescale. Hence, the acid penetrates by convection and diffusion into the domain and reaches the entire pore space. The acid at the solid surface is consumed at a smaller rate leading to near-uniform dissolution pattern. For higher value of the constant rate of reaction, the characteristic time of the dissolution is of the same order of magnitude as the timescale of the transport process. Hence, the reaction activated as soon as the acid reaches the mineral surface. Since the consumption of acid at the surface of the pillars is rapid, the invasion of the acid in the domain is slowed down, which favors the dissolution of the pillars that are closer to the inlet. Once a pillar disappears, it creates a pathway for preferential flow of the acid solution. This phenomenon ultimately leads to the emergence of 'large-scale' wormholes as illustrated in Figure 6b; these observations are in good qualitative agreement with the experiments of Song et al. (2014).

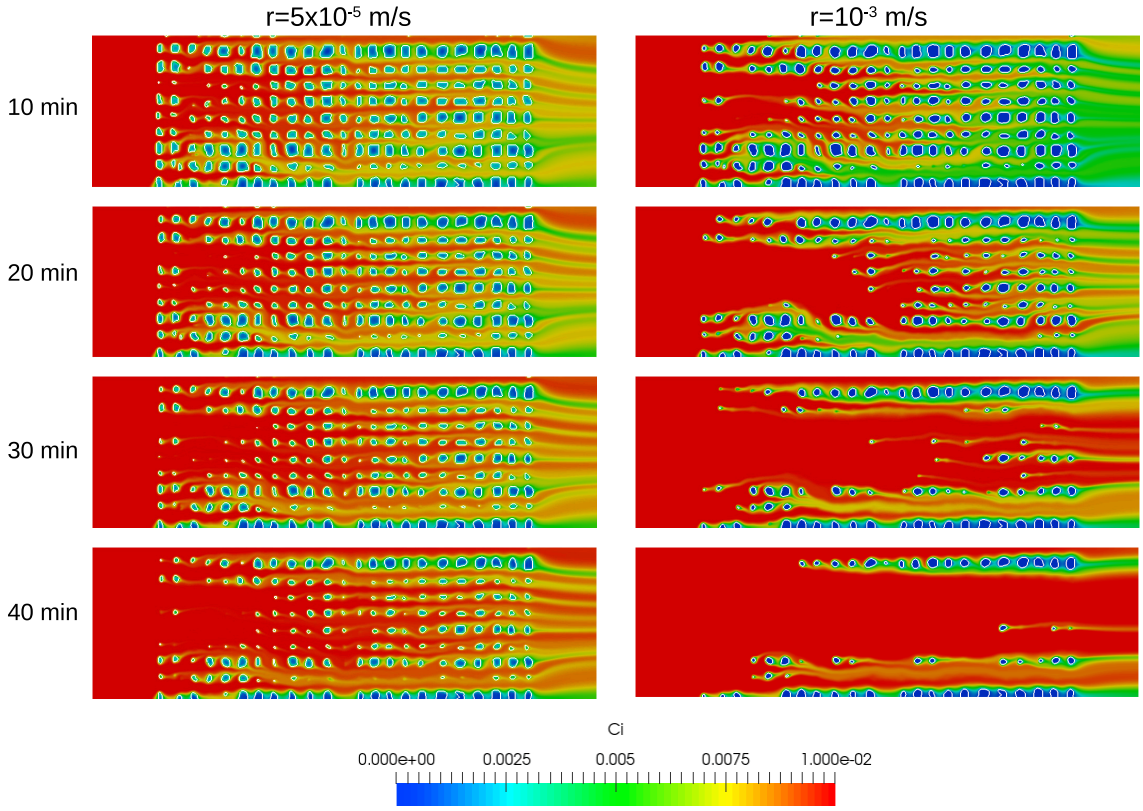

Figure 6 *Evolution of the pore space of a real rock micromodel for different values of the constant of reaction.*

Conclusion

We proposed a micro-continuum formulation based on the Darcy-Brinkman-Stokes (DBS) equation to model dissolution phenomena at the pore scale. Comparison of the DBS results with ALE simulations are in good agreement. The DBS framework was then used to investigate dissolution in micromodels of a 'real' rock. Different nonlinear dissolution regimes are observed for different reaction rates. In particular, for high Damköhler numbers, we observe the emergence of wormholes, which is in agreement with experimental data.

Acknowledgements

We wish to acknowledge the Office of Basic Energy Sciences Energy Frontier Research Center under Contract number DE-AC02-05CH11231, and the TOTAL STEMS project for financial support. We also thank the Stanford Center for Computational Earth & Environmental Sciences (CEES) for computational support.

References

Angot, P., Bruneau, C.H. and Fabrie, P. [1999] A penalization method to take into account obstacles in incompressible viscous flows. *Numerische Mathematik*, **81**(4), 497–520.

Bousquet-Melou, P., Goyeau, B., Quintard, M., Fichot, F. and Gobin, D. [2002] Average momentum equation for interdendritic flow in a solidifying columnar mushy zone. *International Journal of Heat and Mass Transfer*, **45**(17), 3651 – 3665.

Brinkman, H.C. [1947] A Calculation of The Viscous Force Exerted by a Flowing Fluid on a Dense Swarm of Particles. *Appl. Sci. Res.*, **A1**, 27–34.

Békri, S., Thovert, J. and Adler, P. [1995] Dissolution of porous media. *Chemical Engineering Science*, **50**(17), 2765–2791.

Chen, L., Kang, Q., Viswanathan, H.S. and Tao, W.Q. [2014] Pore-scale study of dissolution-induced changes in hydrologic properties of rocks with binary minerals. *Water Resources Research*, **50**(12), 9343–9365.

Cohen, Y. and Rothman, D.H. [2015] Mechanisms for mechanical trapping of geologically sequestered carbon dioxide. In: *Proceedings of the Royal Society of London A: Mathematical, Physical and Engineering Sciences*, 471. The Royal Society, 20140853.

Daccord, G. and Lenormand, R. [1987] Fractal patterns from chemical dissolution. *Nature*, **325**(6099), 41–43.

Fredd, C.N. and Fogler, H.S. [1998] Influence of transport and reaction on wormhole formation in porous media. *AIChE journal*, **44**(9), 1933–1949.

Golfier, F., Zarcone, C., Bazin, B., Lenormand, R., Lasseux, D. and Quintard, M. [2002] On the ability of a Darcy-scale model to capture wormhole formation during the dissolution of a porous medium. *Journal of fluid Mechanics*, **457**, 213–254.

Guo, J., Quintard, M. and Laouafa, F. [2014] Upscaling and large-scale modeling of the dissolution of gypsum cavities. *The 25th International Symposium on Transport Phenomena, 5 November 2014 - 7 November 2014 (Krabi, Thailand)*.

Hsu, C. and Cheng, P. [1990] Thermal dispersion in a porous medium. *International Journal of Heat and Mass Transfer*, **33**(8), 1587–1597.

Huang, H. and Li, X. [2011] Pore-scale simulation of coupled reactive transport and dissolution in fractures and porous media using the level set interface tracking method. *Journal of Nanjing University (Natural Sciences)*, **47**(3), 235–251.

Huber, C., Shafei, B. and Parmigiani, A. [2014] A new pore-scale model for linear and non-linear heterogeneous dissolution and precipitation. *Geochimica et Cosmochimica Acta*, **124**(0), 109 – 130.

Issa [1985] Solution of the Implicitly Discretised Fluid Flow Equations by Operator-Splitting. *Journal of Computational Physics*, **62**, 40–65.

Kang, Q., Chen, L., Valocchi, A.J. and Viswanathan, H.S. [2014] Pore-scale study of dissolution-induced changes in permeability and porosity of porous media. *Journal of Hydrology*, **517**, 1049–1055.

Kang, Q., Zhang, D. and Chen, S. [2003] Simulation of dissolution and precipitation in porous media. *Journal of Geophysical Research: Solid Earth (1978–2012)*, **108**(B10), 1–5.

Khadra, K., Angot, P., Parneix, S. and Caltagirone, J.P. [2000] Fictitious domain approach for numerical modelling of Navier-Stokes equations. *International Journal for Numerical Methods in Fluids*, **34**(8), 651–684.

Li, X., Huang, H. and Meakin, P. [2010] A three-dimensional level set simulation of coupled reactive transport and precipitation/dissolution. *International Journal of Heat and Mass Transfer*, **53**(13), 2908–2923.

Luo, H., Laouafa, F., Debenest, G. and Quintard, M. [2015] Large scale cavity dissolution: From the physical problem to its numerical solution. *European Journal of Mechanics-B/Fluids*, **52**, 131–146.

Luo, H., Laouafa, F., Guo, J. and Quintard, M. [2014] Numerical modeling of three-phase dissolution of underground cavities using a diffuse interface model. *International Journal for Numerical and Analytical Methods in Geomechanics*, **38**, 1600–1616.

Luo, H., Quintard, M., Debenest, G. and Laouafa, F. [2012] Properties of a diffuse interface model based on a porous medium theory for solid-liquid dissolution problems. *Computational Geosciences*, **16**(4), 913–932.

Molins, S., Trebotich, D., Yang, L., Ajo-Franklin, J.B., Ligocki, T.J., Shen, C. and Steefel, C.I. [2014] Pore-scale controls on calcite dissolution rates from flow-through laboratory and numerical experiments. *Environmental science & technology*, **48**(13), 7453–7460.

Oltéan, C., Golfier, F. and Buès, M.A. [2013] Numerical and experimental investigation of buoyancy-driven dissolution in vertical fracture. *Journal of Geophysical Research: Solid Earth*, **118**(5), 2038–2048.

Rathnaweera, T.D., Ranjith, P.G. and Perera, M.S.A. [2016] Experimental investigation of geochemical and mineralogical effects of CO2 sequestration on flow characteristics of reservoir rock in deep saline aquifers. *Scientific Reports*, **6**(19362).

Roman, S., Soulaine, C., AlSaud, M.A., Kovscek, A. and Tchelepi, H. [2015] Particle velocimetry analysis of immiscible two-phase flow in micromodels. *Advances in Water Resources*, –.

Song, W., de Haas, T.W., Fadaei, H. and Sinton, D. [2014] Chip-off-the-old-rock: the study of reservoir-relevant geological processes with real-rock micromodels. *Lab Chip*, **14**, 4382–4390.

Soulaine, C., Gjetvaj, F., Garing, C., Roman, S., Russian, A., Gouze, P. and Tchelepi, H. [2016] The impact of sub-resolution porosity of X-ray microtomography images on the permeability. *Transport in Porous Media*, **113**(1), 227–243.

Soulaine, C. and Tchelepi, H.A. [2016] Micro-continuum approach for pore-scale simulation of subsurface processes. *Transport In Porous Media*.

Steefel, C.I., Molins, S. and Trebotich, D. [2013] Pore Scale Processes Associated with Subsurface CO2 Injection and Sequestration. *Reviews in Mineralogy and Geochemistry*, **77**(1), 259–303.

Szymczak, P. and Ladd, A. [2004] Microscopic simulations of fracture dissolution. *Geophysical research letters*, **31**(23), 1–4.

Szymczak, P. and Ladd, A. [2009] Wormhole formation in dissolving fractures. *Journal of Geophysical Research: Solid Earth*, **114**(B6), 1–22.

Trebotich, D. and Graves, D. [2015] An adaptive finite volume method for the incompressible Navier–Stokes equations in complex geometries. *Communications in Applied Mathematics and Computational Science*, **10**(1), 43–82.

Vafai, K. and Tien, C. [1981] Boundary and inertia effects on flow and heat transfer in porous media. *International Journal of Heat and Mass Transfer*, **24**(2), 195–203.

Vafai, K. and Tien, C. [1982] Boundary and inertia effects on convective mass transfer in porous media. *International Journal of Heat and Mass Transfer*, **25**(8), 1183–1190.

Wakao, N. and Smith, J. [1962] Diffusion in catalyst pellets. *Chemical Engineering Science*, **17**(11), 825–834.

Xu, Z., Huang, H., Li, X. and Meakin, P. [2012] Phase field and level set methods for modeling solute precipitation and/or dissolution. *Computer Physics Communications*, **183**(1), 15–19.